HAL
open science

Transient chirp in high speed photonic crystal quantum dots lasers with controlled spontaneous emission

Remy Braive, Sylvain Barbay, Isabelle Sagnes, Audrey Miard, Isabelle Robert-Philip, Alexios Beveratos

To cite this version:

Remy Braive, Sylvain Barbay, Isabelle Sagnes, Audrey Miard, Isabelle Robert-Philip, et al.. Transient chirp in high speed photonic crystal quantum dots lasers with controlled spontaneous emission. Optics Letters, 2009, pp.554. 10.1364/OL.34.000554 . hal-00345433

HAL Id: hal-00345433

https://hal.science/hal-00345433v1

Submitted on 9 Dec 2008

HAL is a multi-disciplinary open access archive for the deposit and dissemination of scientific research documents, whether they are published or not. The documents may come from teaching and research institutions in France or abroad, or from public or private research centers.

L'archive ouverte pluridisciplinaire **HAL**, est destinée au dépôt et à la diffusion de documents scientifiques de niveau recherche, publiés ou non, émanant des établissements d'enseignement et de recherche français ou étrangers, des laboratoires publics ou privés.

Transient chirp in high speed photonic crystal quantum dots lasers with controlled spontaneous emission

R. Braive, S. Barbay, I. Sagnes, A. Miard, I. Robert-Philip and A. Beveratos

Laboratoire de Photonique et Nanostructures LPN-CNRS UPR-20, Route de Nozay, 91460 Marcoussis, France

**Corresponding author: Alexios.Beveratos@lpn.cnrs.fr*

We report on a series of experiments on the dynamics of spontaneous emission controlled nanolasers. The laser cavity is a photonic crystal slab cavity, embedding self-assembled quantum dots as gain material. The implementation of cavity electrodynamics effects increases significantly the large signal modulation bandwidth, with measured modulation speeds of the order of 10 GHz while keeping an extinction ratio of 19 dB. A linear transient wavelength shift is reported, corresponding to a chirp of less than 100 pm for a 35-ps laser pulse. We observe that the chirp characteristics are independent of the repetition rate of the laser up to 10 GHz. © 2008 Optical Society of America

OCIS codes: 140.3948; 270.5580; 140.5960; 250.5590; 350.4238

Recent progress in the design and fabrication of microcavities [1] has enabled to implement cavity quantum electrodynamics (CQED) effects in solid state. In the weak coupling regime, the acceleration and spatial redistribution of spontaneous emission has recently been exploited in the engineering of non-conventional lasers with high spontaneous emission coupling factors β [2, 3]. Such cavity enhanced lasers promise to have a large direct intensity modulation bandwidth [4]. Large signal modulation bandwidth up to 100 GHz has already been observed with quantum wells photonic crystal lasers [5], although lasing in such structures is strongly affected by high non-radiative recombinations rates with an increase of the laser threshold power [6]. Quantum dots are less sensitive to free surface non-radiative traps thanks to the three-dimensional confinement of carriers. In quantum dots CQED-enhanced lasers, modulation speeds up to 30 GHz are expected [7]. Yet, a major problem in direct modulation semiconductor lasers is the large change of carrier density during pulse emission leading to a detrimental large frequency chirp of the gain-switched pulses. Therefore, it is highly desirable to fabricate a laser yielding minimum chirp for high speed operation. In

this paper, by studying time-resolved spectra and the spectral-resolved temporal evolution of a CQED-enhanced photonic crystal laser embedding quantum dots, we demonstrate that large direct modulation bandwidth up to 10 GHz can be achieved, with a linear spectral chirp of less than 100 pm within the 35 ps pulse width. Linear chirp could be compensated by standard compensation techniques.

The laser cavity is formed by a photonic crystal double heterostructure [1] etched on a 180 nm-thick suspended GaAs membrane and incorporating a single layer of self-assembled InAs quantum dots at its vertical center plane. The whole structure is grown by molecular beam epitaxy. The quantum dot density is of the order of 4.10^{10} cm^{-2} and their spontaneous emission is centered around 945 nm at 4 K with an inhomogeneous broadening of about 30 nm. The cavity is fabricated using electron beam lithography, inductively coupled plasma etching and wet etching [8]. It consists of three segments of W1 photonic crystal waveguides. The intermediate segment extends over two periods with a longitudinal period $a_c = 250$ nm, that is locally enhanced compared to the longitudinal period $a_m = 240$ nm of the two surrounding segments. The targeted air hole-radius r is $0.29\times a_m$.

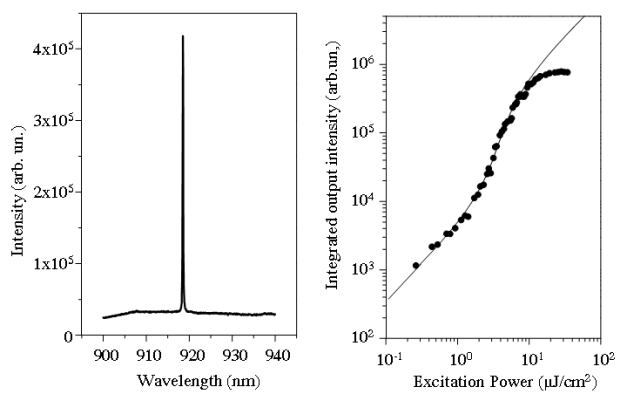

Fig. 1. Left: Laser spectrum of the cavity for an excitation power of 7.76 μJ/cm^2 ($1.7\times P_{th}$) measured onto the surface sample. Right: Integrated output intensity as a function of the excitation power. Full circles: experimental data. Solid line: Rate equation model solution corresponding to β of 0.67.

The cavity is cooled at 4 K. The active material is optically and non-resonantly pumped at normal incidence by a Ti:Sapphire laser delivering 3 ps pulses at a 81.8 MHz repetition rate and tuned to 840 nm near the energy gap of the wetting layer, in order to reduce the impact of thermal heating of the membrane. The pumping laser pulses are focused by a microscope objective (numerical aperture=0.4) onto the sample. The photoluminescence

emitted by the cavity is collected through the same microscope objective and sent on a 32 cm spectrometer ($\simeq$ 0.1 nm resolution) equipped with a cooled silicon charge coupled device. The signal dispersed by the spectrometer is also sent on a Syncroscan streak camera, with a temporal resolution of 3 ps. A typical laser spectrum is shown on Fig. 1a and shows a sharp single-mode lasing peak. Lasing occurs around 920 nm, on the short-wavelength side of the quantum dot spectral distribution as observed in [10]. Cavity modes on resonance with the long-wavelength side of the quantum dot spectral distribution do not display any lasing behavior, since material gain saturation occurs before laser threshold is reached. In order to evidence lasing operation in such cavity, we recorded the integrated output intensity of the cavity mode as a function of pump power. Figure 1(b) shows the resulting Light-in Light-out ($L - L$) curve. A s-shaped smooth intensity transition appears at intermediate excitation levels of the order of P_{th} =4.5 μJ/cm^2. This soft lasing transition has already been observed in CQED-enhanced nanolaser [2,3]. Determination of the spontaneous emission coupling factor β in such cavities is usually obtained from fits of the $L - L$ curve by coupled rate equation models for carrier density N and photon density in the cavity P [2]. Yet, such method leads to a certain degree of uncertainty on the induced value of β, since these equations involve a large number of parameters. Moreover, the output characteristics of such cavity lasers are strongly dependent on the excitation regime [9]. For comparison purpose, $L - L$ curves are fitted to the rate equation model with standard values of the linear gain and transparent carrier density as proposed in [2], we estimate a β factor around factor β =0.67 depicted in solid line in Fig. 1b. We consider a quantum dot lifetime equal to τ_{sp} = 50 ps as measured below threshold (Fig. 2a) corresponding to a Purcell factor of F_p=20 consolidating the high β parameter. For large pumping powers above 6.5 μJ/cm^2, we observe a deviation from the theoretical fit, due to gain saturation effects that are not included in the model.

To investigate the dynamics of our laser, emission from the cavity above and below threshold is analyzed on the streak camera. Typical decay curves are shown on Fig. 2. As expected in CQED enhanced lasers and as already observed in [7], we observe a decrease of the pulse rise time from values of the order of 25 ps below threshold to values of the order to 11 ps for pumping powers of 6.6 μJ/cm^2 (of the order of $1.5P_{th}$), since spontaneous emission rapidly builds up the photon number in the cavity mode. For higher pumping powers ($> 1.5P_{th}$), this rise time is pinned to 11 ps, certainly limited by the capture time. Simultaneously, as the pump rate increases, we observe a strong decrease of the decay time, from 50 ps below threshold to 11 ps above threshold. The minimum decay rate is observed again at pump powers around $1.5P_{th}$ and the decay time remains unchanged for higher pumping rates. This excitation power of $1.5P_{th}$ corresponds to the excitation power at which gain saturation effects appear (see Fig. 1 left). On Figure 2, are also reported the variations of the emission wavelength within the pulse duration, deduced from traces recorded on the streak camera.

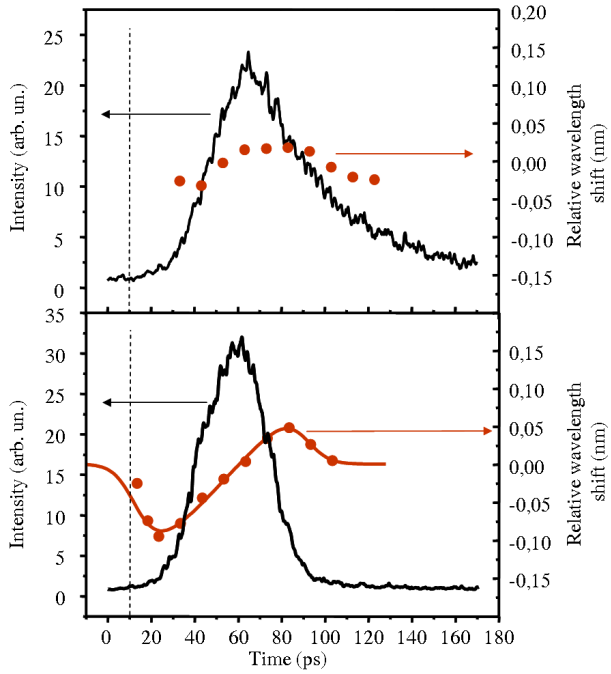

Fig. 2. Time-resolved optical emission from the photonic crystal cavity. (Upper) below the laser threshold ($P \simeq 0.5P_{th}$ =2.1μJ/cm^2), (Lower) above the laser threshold ($P \simeq 5P_{th}$ =22μJ/cm^2). The red circles represent the relative wavelength shift of the spectral maximum intensity as a function of time. Red line corresponds to a fit by Eq. 1. Vertical dashed lines represent the temporal position of the laser excitation pulse.

For low excitation powers below threshold, the wavelength shift is rather small, less than 0.18 $\dot{A}$ within the spectral resolution of the setup. Conversely, well above threshold, we observe a transient chirp, with first a slight blueshift, followed by a continuous linear redshift and then a blueshift. The linear redshift of 100 pm occurs over a time scale of $\Delta\tau = 35$ ps corresponding to the full width at half maximum of the laser pulse. The blueshift results from carrier-induced change of the refractive index, whereas the redshift appears when lasing occurs, decreasing consequently rapidly the total number of carriers. When modeling the delivered temporal laser pulse by a Gaussian-shaped pulse in the form of $e^{-(\frac{t}{\Delta\tau/(2\sqrt{ln2})})^2}$, the laser time-dependent wavelength chirp associated with the dynamic change of the carrier density can be described under large signal modulation by [11]:

$$\delta\lambda(t) = \alpha\frac{\lambda^2}{2\pi c}(\frac{t}{(\Delta\tau/(2\sqrt{ln2}))^2} + \frac{\beta N_{th}}{2\tau_{sp}P}.e^{(\frac{t}{\Delta\tau/(2\sqrt{ln2})})^2}) \quad (1)$$

where α is the linewidth enhancement factor. N_{th} is the carrier density at threshold, P is the maximum photon density in the cavity and τ_{sp} is the spontaneous emission lifetime. When fitting our curve by Eq. 1, the time evolution of the chirp and the small total chirp

are well reproduced, using a fitting parameter N_{th}/P of 0.17 and $\beta = 0.67$. The value of α, equal to 3.05 in this fit, is deduced from time-bandwidth product measurements : $\Delta\nu\Delta\tau = \frac{2ln2}{\pi}\sqrt{1+\alpha^2}$, where $\Delta\nu$ is the full spectral width at half maximum. Such measurements repeated for different excitation powers indicate that α enhances with the pump power [12] from 2.62 up to 3.05, when the excitation power raises from P_{th} to $5P_{th}$. This increase results mainly from the increase of $\Delta\nu$, since $\Delta\tau$ is roughly constant around 35 ps. This enhancement of α may result from gain material saturation effects, inducing low differential gains and thus higher α factors [13]. This α factor value, of the order of the ones observed on quantum well lasers, is large compared to theoretical predictions for quantum dots material gain but rather small compared to the values obtained on conventional quantum dots lasers operating above threshold [14].

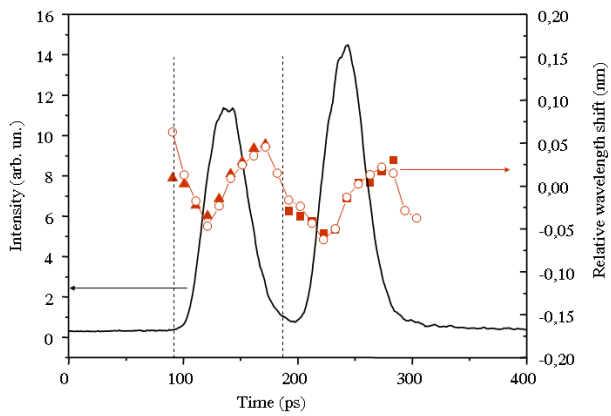

Fig. 3. Temporal and spectral response of the laser cavity excited by two 3-ps pulses separated by 100 ps. The temporal position of the excitation pulses are indicated by vertical dash lines. The excitation power is set to $5P_{th}$. The chirp has been measured, when the device is excited by only the first (full triangles), only the second (full squares) or both excitation pulses (circles).

When applying a direct large-signal modulation to the device, it is important that all pulses delivered at high repetition rate present the same linear wavelength dependency, allowing for an effective group velocity dispersion compensation independently of the modulation pattern. Figure 3 presents the temporal response of our laser, when excited by two subsequent 3-ps pulses separated by 100 ps. The response of the laser follows the pump with a clear 19 dB extinction rate between the two pulses: the photonic crystal laser delivers two identical 34 ps width pulses with a time difference of 100 ps. The spectral variation of the optical frequency has also been measured, when the sample is pumped by only one of the two excitation

pulses and when the sample is pumped by the two subsequent excitation pulses. We observe that the chirp is identical in the two-pulse excitation regime to that observed in the one-pulse excitation regime for each pulse. Moreover, in the two-pulse excitation regime, the variations of the wavelength during the pulses duration, are identical in both pulses. This result indicates that the whole system has relaxed on a time scale smaller than 100 ps, since the characteristics of the second pulse are not affected by the first one.

In summary, the spectral response in time of modulated CQED enhanced lasers at large-signal direct modulation rates of 10 GHz has been investigated. Our results indicate a small linear transient chirp within each pulse duration, that could be compensated by use of highly dispersive single-mode fibres. The chirp characteristics of subsequent delivered pulses do not depend on the direct modulation bandwidth up to 10 GHz. These results confirm that quantum dot photonic crystal lasers with high spontaneous emission coupling factors may improve significantly technologies for high pulse repetition rate applications such as optical interconnections.

The authors would like to thank A. Lemaître for samples growth as well as R. Kuszelewicz and P. Voisin for useful discussions. The authors also thank K. Meunier and J. Bloch for lending critical electronic equipment.

References

1. B.-S. Song, S. Noda, T. Asano and Y. Akahane, "Ultra-high-Q photonic double heterostructure nanocavity," Nature Materials**4**, 207 (2005).
2. S. Strauf, K. Hennessy, M. T. Rakher, Y.-S. Choi, A. Badolato, L. C. Andreani, E. L. Hu, P. M. Petroff and D. Bouwmeester, "Self-Tuned Quantum Dot Gain in Photonic Crystal Lasers," Phys. Rev. Lett. **96** 127404 (2006).
3. S. M. Ulrich, C. Gies, S. Ates, J. Wiersig, S. Reitzenstein, C. Hofmann, A. Löffler, A. Forchel, F. Jahnke and P. Michler, "Photon Statistics of Semiconductor Microcavity Lasers," Phys. Rev. Lett. **98** 043906 (2007).
4. Y. Yamamoto, S. Machida and G. Björk, "Microcavity semiconductor laser with enhanced spontaneous emission," Phys. Rev. A **44**, 657 (1991).
5. H. Altug, D. Englund and J. Vuckovic, "Ultrafast photonic crystal nanocavity laser," Nature Physics **2**, 484 (2006).
6. D. Englund, H. Altug, J. Vuckovic, "Low-threshold surface-passivated photonic crystal nanocavity laser," Appl. Phys. Lett. **91**, 071124 (2007).
7. B. Ellis, I. Fushman, D. Englund, B. Zhang, Y. Yamamoto and J. Vuckovic, "Dynamics of quantum dot photonic crystal lasers," Appl. Phys. Lett. **90**, 151102 (2007).
8. R. Braive, L. LeGratiet, S. Guillet, G. Patriarche, A. Miard, A. Beveratos, I. Robert-Philip and I. Sagnes, "Inductively Coupled Plasma etching of GaAs suspended photonic

crystal cavities," submitted J. Vac. Sci. Technol. B

9. C. Gies, J. Wiersig and F. Jahnke, "Output Characteristics of Pulsed and Continuous-Wave-Excited Quantum-Dot Microcavity Lasers," Phys. Rev. Lett. **101**, 067401 (2008).
10. Z. G. Xie, S. Götzinger, W. Fang, H. Cao and G. S. Solomon, "Influence of a Single Quantum Dot State on the Characteristics of a Microdisk Laser," Phys. Rev. Lett. **98**, 117401 (2007).
11. F. Koyama and Y. Suematsu, "Analysis of Dynamics Spectral Width of Dynamic-Single-Mode (DSM) Lasers and Related Transmission Bandwidth of Single-Mode Fivers," IEEE J. Quantum Electron. **21**, 292 (1985)
12. S. Melnik, G. Huyet and A. Uskov, "The linewidth enhancement factor a of quantum dot semiconductor lasers," Opt. Express **14**, 2950 (2006).
13. J. Muszalski, J. Houlihan, G. Huyet and B. Corbett, "Measurement of linewidth enhancement factor in self-assembled quantum dot semiconductor lasers emitting at 1310 nm," Electron. Lett. **40**, 428 (2004).
14. A. Markus, J. X. Chen, O. Gauthier-Lafaye, J.-G. Provost, C. Paranthoën and A. Fiore, "Impact of intraband relaxation on the performance of a quantum-dot laser," IEEE J. Select. Topics Quantum Electron. **9**, 1308 (2003).